Matching Persistent Scatterers to Optical Oblique Images

Lukas Schack
Leibniz Universität Hannover
Institute of Photogrammetry and GeoInformation
schack@ipi.uni-hannover.de

Uwe Soergel
Technische Universität Darmstadt
Institute of Geodesy
soergel@geod.tu-darmstadt.de

Abstract

Persistent Scatterer Interferometry is a well established method for subsidence monitoring of buildings especially in urban areas. Even though the very high resolution of current SAR missions allow for ground resolutions of some decimeters, the assignment of Persistent Scatterers to single parts of buildings is not well investigated yet. We present a new approach how to incorporate optical oblique imagery to assign Persistent Scatterers to their presumed correspondences in the optical data in order to establish a link between Persistent Scatterers and single structures of buildings. This is a crucial step for advanced subsidence monitoring in urban ares. The centerpiece of the presented work is a measure which quantifies the quality of the bipartite matching between single Persistent Scatterers and their correspondences at a regular lattice in the optical data. The applicability of our approach is presented in two exemplary case studies.

1. Introduction

Synthetic Aperture Radar (SAR) is the principal source for weather and sunlight independent remotely sensed information about the earth. Especially the analysis of time series offer indispensable insights into the movement characteristics of urban areas and provide the basis for monitoring tasks at the scale of some mm per year. Persistent Scatterer Interferometry (PSI) considers only temporally stable and dominant scatterers which are often induced by man made structures like window corners or balconies [6]. Those structures form trihedral corners which directly retroreflect the signal back to the sensor. For modern SAR sensors like TerraSAR-X a side length of some cm of such trihedral reflectors is sufficient to induce very strong and easily to detect Persistent Scatterers [3]. Even though the reflection properties for simple geometric forms are understood in satisfying detail and can also be simulated [1], the PSI processing is still an opportunistic method. To use it systematically for reliable applications like, for instance, building monitoring in subsidence areas, the scattering mechanisms have to be understood in more detail.

In this paper, we present a method how to incorporate an additional source of information to gain more knowledge about Persistent Scatteres (PS) at facades. Since the assignment of single PS to their correspondences in optical imagery is very complicated due to the quite different sensing characteristics, we exploit the regular alignment of windows at facades and establish the link to optical oblique imagery of the same buildings on the basis of lattices representing the facade. Since the imaging geometry of optical oblique imagery is also capturing the facades of buildings it lends itself as a reference to find correspondences of Persistent Scatterers. In contrast to point-wise targets as the result of PSI, the image offers two-dimensional extensive information about the direct neighborhood of a Persistent Scatterer which can easily be analyzed. Our aim in this paper is rather to establish this relationship than performing an exhaustive interpretation of the behavior of PS at facades. We formulate the assignment of PS to the equivalent parts of the image as finding an maximal bipartite matching considering a problem specific matching distance measure. A quantified measure of the matching quality is derived and allows for a qualified interpretation of the fused result. We also give two examples for the applicability and interpretability of the presented approach.

To make a reliable statement about the localization accuracy of PS in optical images one has to take into account the anisotropic error budget of the SAR sensor. While the range and azimuth direction can be determined within cm accuracy, the third coordinate, i.e. elevation direction, can only be determined within some decimeter accuracy for typical sensing configurations [2]. This leads to strong correlations between the coordinates when transferred to a global reference coordinate system. We also show how the consequences of this anisotropic behavior can be mitigated by incorporating prior knowledge about the distribution of PS at facades.

1.1. Related Work

An overview over applications of PSI with a focus on subsidence monitoring of urban areas is given in [5]. There are many approaches to fuse SAR data with optical imagery. The joint data analysis is mostly done using time series to classify land cover, *e.g.* [4], [17]. [16] uses line features in SAR and optical nadir images to establish the correspondence. First investigations regarding the regularity of Persistent Scatterers at building facades are presented in [15]. Instead of lattices only horizontal lines of PS were considered. The benefit of grouping PS for their common height is derived. We continue this approach and expand it to group all three coordinate directions instead of only one. The approach proposed in [8] incorporates three dimensional building models which are derived by densely matched images from an UAV to evaluate the localization accuracy of PS at facades. Our approach aims at a similar direction but explicitly exploits the regular alignment of PS at facades.

1.2. Model based data matching

To jointly describe data originating from two physically and geometrically different sensors a common reference system and data representation is necessary. We apply a model which can be implicitly described by four fundamental assumptions which are stated in the following.

1. **All PS at a facade are situated in a plane.** We exploit the every day experience that facades can usually be approximated by planes. This holds for the majority of facades in densely developed city centers with many office and other high-rise buildings.

2. **The optical image and the projection into it is seen as accurate reference.** We assume the optical imagery as free from errors. Also the projection from three-dimensional object coordinates into the image is modeled to be errorless. The accuracy of a projected point is therefore governed solely by the positioning error of the PS in object space.

3. **PS at the facade are induced by the same, repetitive geometric structure and their appearance in an optical image is the same.** The appearance of the neighborhood in the optical image is the same for every PS belonging to this regular pattern at the facade.

4. **The geometrical structure causing the PS is visible in the image.** To adduce the image as an additional source of information in the process of understanding the physical nature of PS, the part of the facade structure causing the PS has to be visible in the image. More precisely, the structure has to be distinguishable from the background in terms of a high contrast or a specific outline. Since oblique imagery is usually captured with a camera system pointing at all four cardinal directions, the facade should be depicted in at least one image.

Instead of dealing with every PS separately we consider sets of PS as representations of facades objects. According to our model the set of PS belonging to one facade can be described as a lattice

$$L := \{a \cdot t_1 + b \cdot t_2 + t_3\}$$
$$\text{with: } [0, a_U] := \{a \in \mathbb{N} | a \leq a_U\} \quad (1)$$
$$[0, b_U] := \{b \in \mathbb{N} | b \leq b_U\}$$

where t_1 and t_2 are the lattice spanning vectors defining the spacing and direction of consecutive points along the horizontal and vertical alignment direction of facade structures. t_3 can be interpreted as the origin of the lattice. The repetitions are reflected in the natural numbers a and b (including 0) which are bounded by the upper limits a_U and b_U.

1.3. Bipartite matching

As we are interested in the correspondences for all PS at a facade in an optical image we aim at establishing an one to one assignment between the PS and the point-wise representation of PS inducing geometrical structures in the image. In other words, one has to ensure that no two PS are assigned to the same lattice node or vice versa. This assignment problem can be formulated as finding the maximal matching in a bipartite graph $G = (V, E)$ where the PS and the nodes of a lattice representing the regularity in the image are two disjoint groups of vertices: $V = \{P, L\}, P \cap L = \emptyset$ where P denotes all PS projected into the oblique image and L are the lattice nodes defined by (1). The weighted edges $E = P \times L$ correspond to the assignment of the PS and lattice nodes adjacent to these edges. A matching is a subset $M \subseteq E$ of edges between P and L where no vertex is adjacent to more than one edge. This ensures the one to one correspondence. A maximum matching means that as many edges as possible between P and L exist. Such assignment problem is a standard task in combinatorial theory and can be exactly solved by the Hungarian algorithm [12]. Figure 1 shows the basic principle of bipartite graph matching. The matching result is marked with thick lines. Note that usually the proposed lattice L consists of more points than PS, thus, $|L| > |P|$ and, therefore, many lattice points stay unmatched while all PS are assigned to lattice points.

2. Data Preprocessing

In order to reference Persistent Scatterers to optical oblique images both data types have to be transferred into a single reference system. Following assumption (2) we consider the oblique image as the reference and the projection of a three-dimensional object coordinate into it as
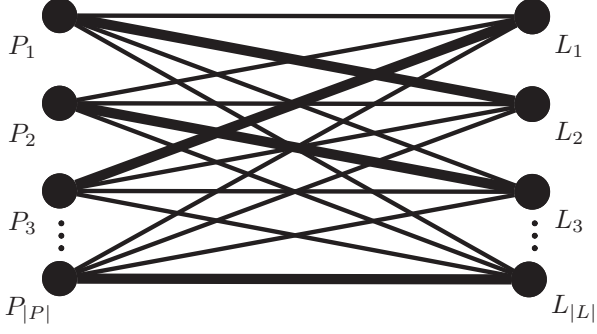
Figure 1: Principle of bipartite matching. On the left hand side all $|P|$ Persistent Scatterers are sketched as one part of the bipartite graph. The lattice nodes L_1 to L_M form the other part. Among all possible $|P| \times |L|$ edges (depicted as thin lines) the biggest possible subset yielding the smallest sum of edge weights is the solution of the bipartite matching (marked as thick lines).

error-free. Furthermore, it is well known that the two-dimensional SAR image coordinates range and azimuth are orders of magnitude more precise than the third dimension, elevation. The regular distribution of PS in terms of regular patterns can therefore better be captured in the SAR domain.

Consequently, our aim for the data preprocessing is, on the one hand, to extract topology information from the Persistent Scatterers in the SAR domain and, on the other hand, to transfer them and their covariance matrix into the image space.

2.1. Improving the PS positioning accuracy

Given a set of Persistent Scatterers in range and azimuth coordinates as well as in geocoded world coordinates we first segment them into single facades. In order to do so, the normal of the local plane through the 10 nearest neighbors at every PS is clustered to distinguish different facade orientations. To further separate facades of the same orientation the mutual Euclidean distance is used assuming that the difference between points belonging to the same facade is smaller than the distance between PS of different facades. The procedure is inspired by [14] and the reader is referred thereto for more details.

A single two-dimensional SAR acquisition has the coordinate axis corresponding to the flight direction of the satellite (azimuth) and the sensing direction (range). The accuracy of these two SAR coordinates is largely determined by the sensing hardware. Using a stack of acquisitions allows for resolving the third coordinate direction (elevation), however, with a notably worse accuracy. The experiments in this paper are conducted on a set of Persistent Scatterers derived from a stack of $N = 54$ TerraSAR-X High-Resolution
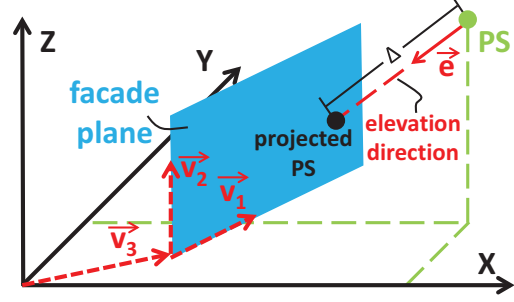

Figure 2: Sketch of the plane projection procedure. The PS marked in green is projected onto the robustly estimated plane (shown in blue) along the elevation direction.

Spotlight acquisitions. According to the parameters of the stack we yield lower bounds for the theoretical localization precision in the SAR domain ([3]) of

$$\sigma_{az} \approx \frac{0.55}{\sqrt{\text{SNR} \cdot N}} \cdot \rho_{az} = 0.020m$$

$$\sigma_{rg} \approx \frac{0.55}{\sqrt{\text{SNR} \cdot N}} \cdot \rho_{rg} = 0.035m \qquad (2)$$

$$\sigma_{el} \approx \frac{\lambda R}{4\pi \cdot \sqrt{2\,\text{SNR} \cdot N} \cdot \sigma_B} = 0.6m$$

where SNR denotes the signal-to-noise ratio of a dominant scatterer with respect to the surrounding clutter, R the distance from sensor to the object, σ_B the standard deviation of the perpendicular baseline of the acquisitions, the wavelength λ, and finally ρ_{az} and ρ_{rg} the resolution in azimuth and range direction of the SAR system, respectively. The discrepancy of factor ~ 30 is salient.

The SAR coordinates $\overrightarrow{P_{RAE}}$ can be transformed into real world coordinates by applying two rotations around the Z-axis (heading angle t_{az} of the SAR sensor) and Y-axis (incidence angle θ), respectively:

$$f : \overrightarrow{P_{XYZ}} = R_z(t_{az})^T \cdot R_y(\theta)^T \cdot \overrightarrow{P_{RAE}}. \qquad (3)$$

To obtain the covariance matrix Σ_{XYZ} one can apply standard error propagation [11] by differentiating these transformation:

$$\Sigma_{XYZ} = F\Sigma_{RAE}F^T \qquad (4)$$

where F contains the partial derivatives of f with respect to the PS coordinates in the SAR domain. The resulting covariance matrix Σ_{XYZ} has the form

$$\Sigma_{XYZ} = \begin{bmatrix} \sigma_X^2 & \sigma_{XY} & \sigma_{XZ} \\ & \sigma_Y^2 & \sigma_{YZ} \\ \text{sym.} & & \sigma_Z^2 \end{bmatrix}$$

$$= \begin{bmatrix} C(\sigma_R^2 + \sigma_A^2 + \sigma_E^2) & C(\sigma_A^2 - \sigma_R^2) & C(\sigma_E^2 - \sigma_R^2) \\ & C(\sigma_R^2 + \sigma_A^2 + \sigma_E^2) & C(\sigma_E^2 - \sigma_R^2) \\ \text{sym.} & & C(\sigma_R^2 + \sigma_E^2) \end{bmatrix}$$

$$(5)$$

where C is a placeholder for any trigonometric function of the two angles t_{az} and θ. From the structure of the covariance matrix it can be seen that the correlations between the coordinates in the object system gets higher, the bigger the discrepancy between the error budget of the elevation direction σ_E relative to the range direction σ_R becomes.

To mitigate this anisotropic error behavior, we apply model assumption (1) (all PS of a facade are situated in a plane) by fitting an adjusted RANSAC plane [7] through all PS belonging to the same facade. All PS are then projected onto this plane along the elevation direction. Figure 2 shows this procedure schematically. Given the plane defining vectors $\{\vec{v_1}, \vec{v_2}, \vec{v_3}\}$ and the three-dimensional position of the PS $\overrightarrow{P_{XYZ}}$ the intersection point of the plane with the elevation direction fulfills the equation

$$\overrightarrow{P_{XYZ}} + \Delta \vec{e} = \vec{v_3} + r\vec{v_1} + s\vec{v_2} \qquad (6)$$

where Δ is the distance from the PS to the plane in elevation direction. Solving this equation for the triplet $\{\Delta, r, s\}$ and plugging it in the right hand side of equation 6 yields the projected coordinates of the PS in the XYZ space.

We then exploit the topology of the grouping results in section 2.1 by explicitly forming groups of H horizontally or V vertically aligned PS. Looking upon H horizontally aligned PS can be seen as H times measuring the same height [15], assuming zero mean and equally precise measurements. We extend this approach by also averaging the planimetric position, i.e. X and Y coordinate, of V vertically aligned PS:

$$g_1 : \overline{X} = \frac{1}{H}\sum_{i=1}^{H} X_i \quad \text{and} \quad g_2 : \overline{Y} = \frac{1}{H}\sum_{i=1}^{H} Y_i$$
$$g_3 : \overline{Z} = \frac{1}{V}\sum_{i=1}^{V} Z_i \qquad (7)$$

Taking into account that not all PS of a $H \times V$ lattice are present due to temporal decorrelation or occlusion, for instance, the averaged group coordinates can be interpreted as a lower bound for the covariance matrix. The grouped covariances are then

$$\overline{\Sigma_{XYZ}} = G\Sigma_{XYZ}G^T$$
$$= \begin{bmatrix} \sigma_X^2/H & \sigma_{XY}/H & \sigma_{XZ}/V \\ & \sigma_Y^2/H & \sigma_{YZ}/V \\ \text{sym.} & & \sigma_Z^2/V \end{bmatrix} \qquad (8)$$

with G containing the partial derivatives of g_1, g_2 and g_3 with respect to X, Y, and Z. Comparing the covariance matrix of the averaged PS (8) with the original covariance matrix (5) shows directly that the latter is smaller by a factor of $\frac{1}{H}$ or $\frac{1}{V}$, respectively. The impact of this individual grouping and, therefore, individual covariance matrices is
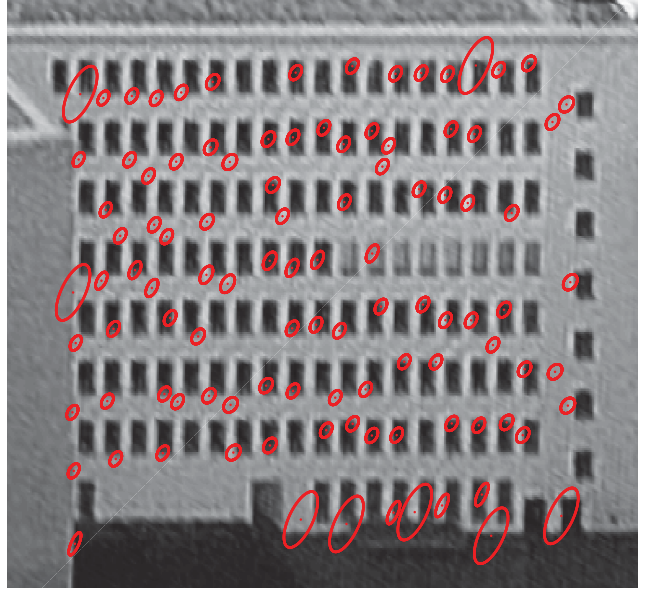

Figure 3: A rectified facade with 95% error ellipses of the propagated positioning accuracy. Differently sized ellipses are a result of the individual grouping.

exemplarily shown in Figure 3. In red the 95% confidence level error ellipses are drawn. The PS on the ground level could not be grouped and therefore exhibit a bigger uncertainty.

The remaining transformation is the projection of the grouped PS into an optical oblique image. This is done by applying the standard collinearity equations. Following assumption (2), we consider this projection error-free. Building the partial derivatives with respect to the averaged object coordinates and multiplying it with $\overline{\Sigma_{XYZ}}$ in the same way like before yields an covariance estimation for the localization accuracy for grouped PS in the oblique image.

3. Method

Our aim is to find the maximal bipartite matching between the projected Persistent Scatterers and lattice nodes describing the underlying regularity in the optical image. The matching costs are defined by quantifying the model assumptions mentioned in section 1.2.

3.1. Lattice proposal

A crucial step in the presented approach is the proposal of matching partners for the Persistent Scatterers. Following equation (1) the set of lattice points L in the image is determined by the two spanning vectors t_1 and t_2, the lattice origin t_3, and upper bounds for the extent a_U and b_U. Implementing the model assumptions of section 1.2 and exploiting preliminary results from the preprocessing

lets us narrow down the search space of possible lattices. We achieve this by the following steps.

3.1.1 Image rectification

According to assumption (1) all PS at a facade lie in one plane. This plane is robustly estimated during the preprocessing in three-dimensional object space. Given the orientation parameters of the oblique image, the direction between the plane normal and the camera's viewing angle can be computed. Projecting this direction into the image allows to rectify the image in a way that the horizontal alignment of facade objects corresponds to one image coordinate axis while the other coincides with the vertical alignment. This reduces the two-dimensional spanning vectors t_1 and t_2 to scalar values with values corresponding to the horizontal and vertical lattice spacing in the rectified image, respectively.

3.1.2 Spacing estimation

Following assumptions (3) and (4) of our model the geometrical structures inducing the Persistent Scatterers are a repetitive pattern which is discernible in the oblique image. In the proposed model the repetitions occur with constant spacings in horizontal and vertical direction of the facade. We use the well established cross-correlation procedure to extract this regularity. The approximate size of the matching template can be derived from the previously performed grouping of the PS. Since the geometrical structure inducing the PS at the facade has a certain extent in the image the actual template size is robust and still capturing the regularity even if it is slightly under or over-estimated.

Since we work on rectified images, the spacings in X and Y direction can be extracted independently from each other. In order to do so, we apply a voting scheme for the differences of local maxima of the normalized cross correlation result. Taking the maximum of peak differences is a robust estimate for the spacing and empirically yields very reliable results. To derive a measure on how well a lattice node conforms the regularity assumption (3) the correlation coefficient is computed for every lattice node L_m of the matched pairs in M.

3.2. Origin estimation

Having extracted the regularity of the facade image we aim at extracting the part of the regular patch which most likely induces the PS. In terms of equation (1) every lattice defining parameter except the origin t_3 and the lattice extent a_U and b_U are determined. Since the bipartite matching ensures a one-to-one assignment of PS to lattice nodes, the actual extent of the 'true lattice' is implicitly limited. We focus now on finding the most likely origin of the lattice
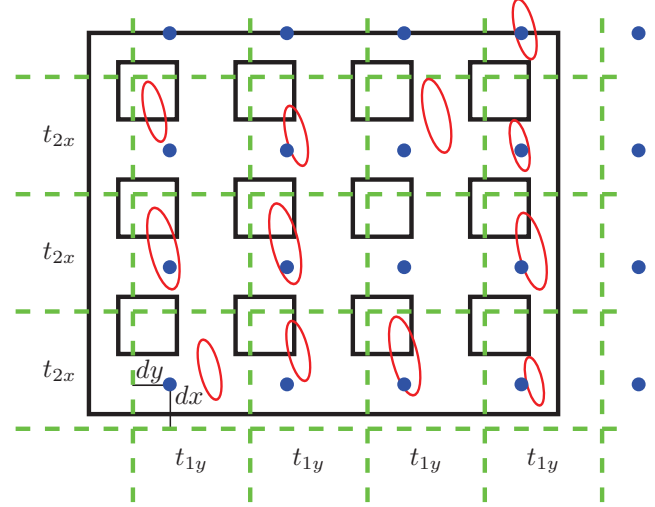

Figure 4: Sketch of the rectified facade model. The green dashed lines are equally spaced according to the spacing estimation based on cross correlation. The red ellipses symbolize the error ellipses of the projected PS. The blue lattice nodes are determined by the offset (dy, dy). An optimal solution minimizes the Mahalanobis distance between matched pairs of lattice nodes and PS.

which means to find the most likely pixel inside the regular patch. Figure 4 shows schematically the rectified facade image. The dashed green lines are the spacings according to the maximum peaks in the cross correlated result. The remaining parameter to estimate (t_3) can be interpreted as the translation between the lattice points (blue points) and the intersections of the green dashed spacing lines. Due to the repetitive manner of the lattice model, the origin can be independently estimated in every regular patch. We denote this translation as dy in horizontal and dx in vertical direction, respectively, and hence, $t_3 = [dy, dx]^T$.

The distance between the set of lattice points L defined by the parameters and the corresponding PS projected to the image should be small. As mentioned above, the anisotropy of the error budget has to be taken into account leading to correlated coordinates in the image and therefore to elliptic isolines of points with the same distance in the anisotropic error metric. We choose the lattice origin (dx, dy) which minimizes the distance for every pair of matched lattice point and assigned PS according to the Mahalanobis distance [10]. The distance $\delta(m)$ between a matched pair m of PS and the corresponding lattice point, i.e. the vertices adjacent to an edge m of the matching M, is defined as

$$\delta(m) = \sqrt{(\overrightarrow{L_m} - \overrightarrow{P_m})\Sigma_{xy,m}^{-1}(\overrightarrow{L_m} - \overrightarrow{P_m})^T} \quad (9)$$

where $\overrightarrow{L_m}$ are the coordinates of the lattice point and $\overrightarrow{P_m}$ is the matched PS, respectively. Note that the covariance

matrix $\Sigma_{xy,m}$ is not the same for every PS due to the PS-individual grouping results. In Figure 4 this is indicated by differently sized error ellipses. The Mahalanobis distance captures well the anisotropy of the error budget and is inexpensive to compute.

The overall score which we want to minimize is than defined as the sum over all distances between matched pairs

$$\hat{t_3} = \operatorname*{argmin}_{t_3} \sum_{m:M \subseteq E(t_3)} \delta(m) \qquad (10)$$

where m is the index over all matchings of PS and lattice nodes. The lattice nodes are dependent on the lattice origin t_3 which implies that t_3 has to be set prior to evaluating the distance measure. Even though the search space for dx and dy is limited by $0 \le dy \le t_{1y}$ and $0 \le dx \le t_{2x}$, respectively, applying a search strategy is beneficial in terms of lowering the computational effort (The Hungarian algorithm has a complexity of $\mathcal{O}\left((|P| + |L|)^3\right)$. Therefore, we apply a standard simplex search method based on the Nelder-Mead algorithm [9].

4. Interpreting the matching result

The matched result can be interpreted twofold: The intentional viewpoint is to derive a quantitative measure of how well the Persistent Scatterers can be assigned to their correspondences in an optical oblique image. Another way of interpreting the presented method is to understand it as a fusion result and use the combined information, for instance, to improve the Persistent Scatterer processing. This could be done by identifying lattice nodes which are not matched to a Persistent Scatterer despite having strong support in the optical data which means that the regular structure inducing PS at other lattice positions is apparently present at that position. For both outlined scenarios a quantitative measure is helpful. We assess the model quality by combining the matching costs which is the summed Mahalanobis distances as outlined in equation (9) as well as the correlation coefficient for every matched lattice node. To make both values comparable, we assume that the underlying distribution of matched PS is bimodal and the problem can, therefore, be seen as a binary classification problem. Either a PS belongs to the regular structure at the facade or not. The same holds for the lattice nodes. Either a lattice node and its surrounding represents the underlying regularity or not. Therefore we apply the thresholding approach of [13] to separate the following four classes in total:

- **A lattice node has support from both data types.** The lattice node is centered in an area which complies with the regularity assumption (3) (high correlation coefficient) as well as the Mahalanobis distance to the corresponding Persistent Scatterer is small. These points can be interpreted as good matches where the

presented model seems to be right. In the following case studies those lattice nodes are marked in green.

- **A lattice node has support only from PS data.** The Mahalanobis distance to a PS is small but the underlying regularity is not present. This could be due to a validation of model assumption (4) (PS inducing structure is visible in the image). Reflections or occlusions lead to such behavior. Since the viewing directions between both sensor types are different, some parts of a facade can be visible in one type of data but not in the other. Such points are marked in red.

- **A lattice node has support only from optical data.** The lattice node has a strong correlation coefficient but no PS is close in terms of the Mahalanobis distance. These nodes are interesting for further investigations with respect to the PS processing. Since the optical appearance of this node's neighborhood is the same as that of similar nodes with PS support and applying model assumption (3) (PS are induced by the same geometrical structure) the lattice information could be used to infer missing PS on such positions. Nodes of this kind are marked in blue.

- **A lattice node has no support neither from PS nor optical data.** Those points are discarded and marked in gray.

5. Case studies

We show two examples of possible applications of the presented approach. No quantitative evaluation of the results can be performed due to the missing ground truth information.

5.1. Axel-Springer building

The Axel-Springer building is an example for a typical high-rise office building in densely developed city centers. It is a 19-storied tower of 78 meters total height. The facade exhibits regularly aligned vertical and horizontal braces. Figure 5 shows four processing steps of the presented approach. In 5a the support of the optical data is shown. The lattice nodes are the final result of the Nelder-Mead algorithm and are the same in the following figures. The color codes the normalized cross correlation between every patch centered at every lattice point and the mean patch of matched lattice nodes. In the lower middle part of the facade an area of low support can be identified. This is due to the different appearance of the facade in this area due to a reflection of another building. In Figure 5b the support by the PS data according to the Mahalanobis distance is color coded. The value is also normalized to make it comparable (visually and numerically) with the optical score. For reasons of visual clarity the original positions of PS are omitted

(a) support from optical data

(b) support from PS data

(c) classification into four groups
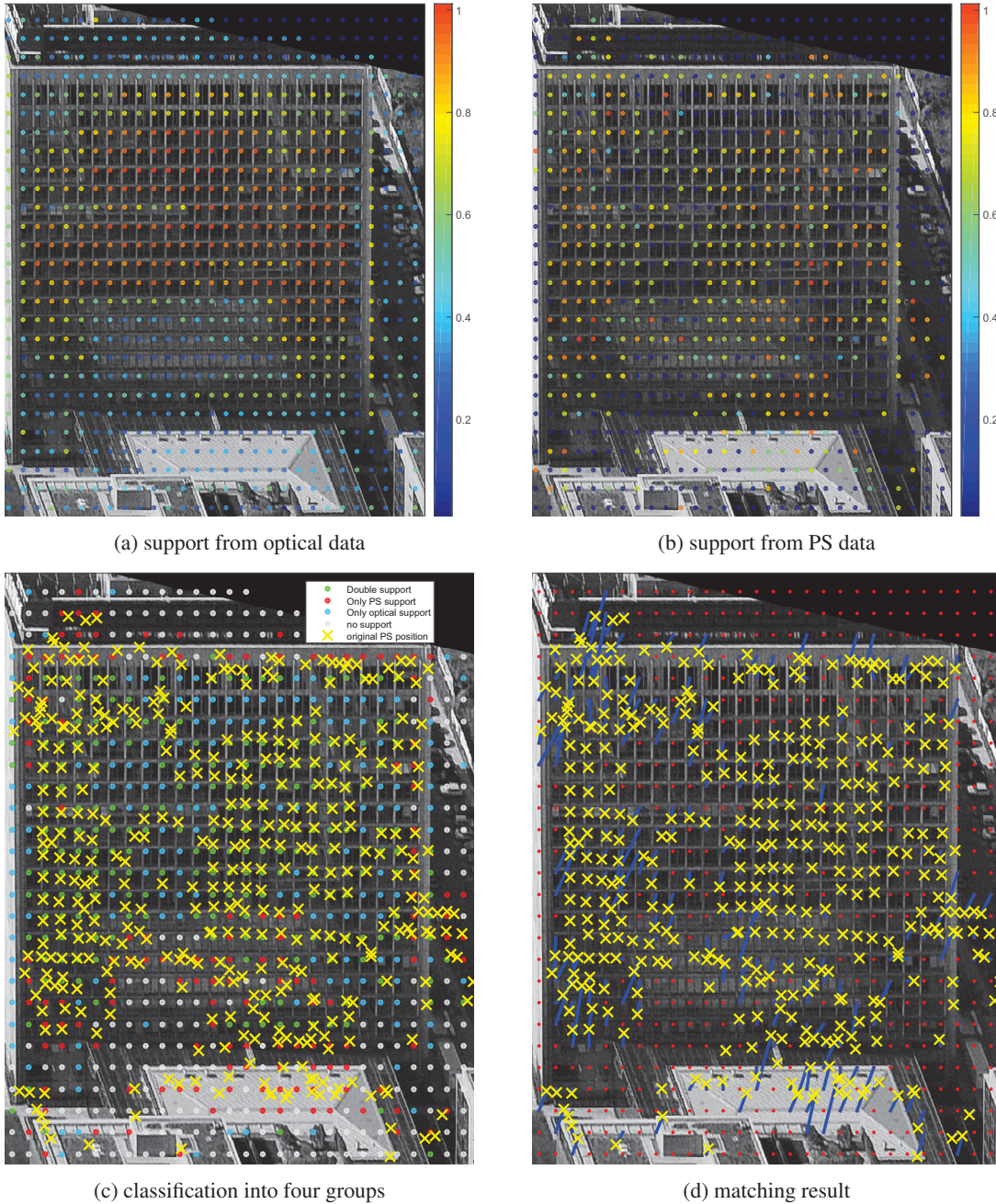
(d) matching result

Figure 5: Result for case study 'Axel-Springer building'. (a) shows the support by the optical data. The color codes the normalized correlation coefficient for the neighborhood around every lattice node compared to the mean patch. (b) shows the support by the Persistent Scatterer data. For reasons of clarity the original positions of the PS are omitted but can be seen in (c). (c) depicts the classified result where the color of the lattice nodes codes the class affiliation according to the legend. The original positions of the PS are marked with yellow crosses. In (d) all matched pairs are linked with blue lines.

here but can be seen in Figure 5c. A violation of the model assumption (2) (projection into the image is error-free) can be identified by looking to the right hand side next to the building. Some PS are projected onto the image but can-not be assigned to the facade. The four colors represent the classes as described in section 4. Figure 5d finally shows the matching result as blue lines between adjacent nodes and PS, respectively.
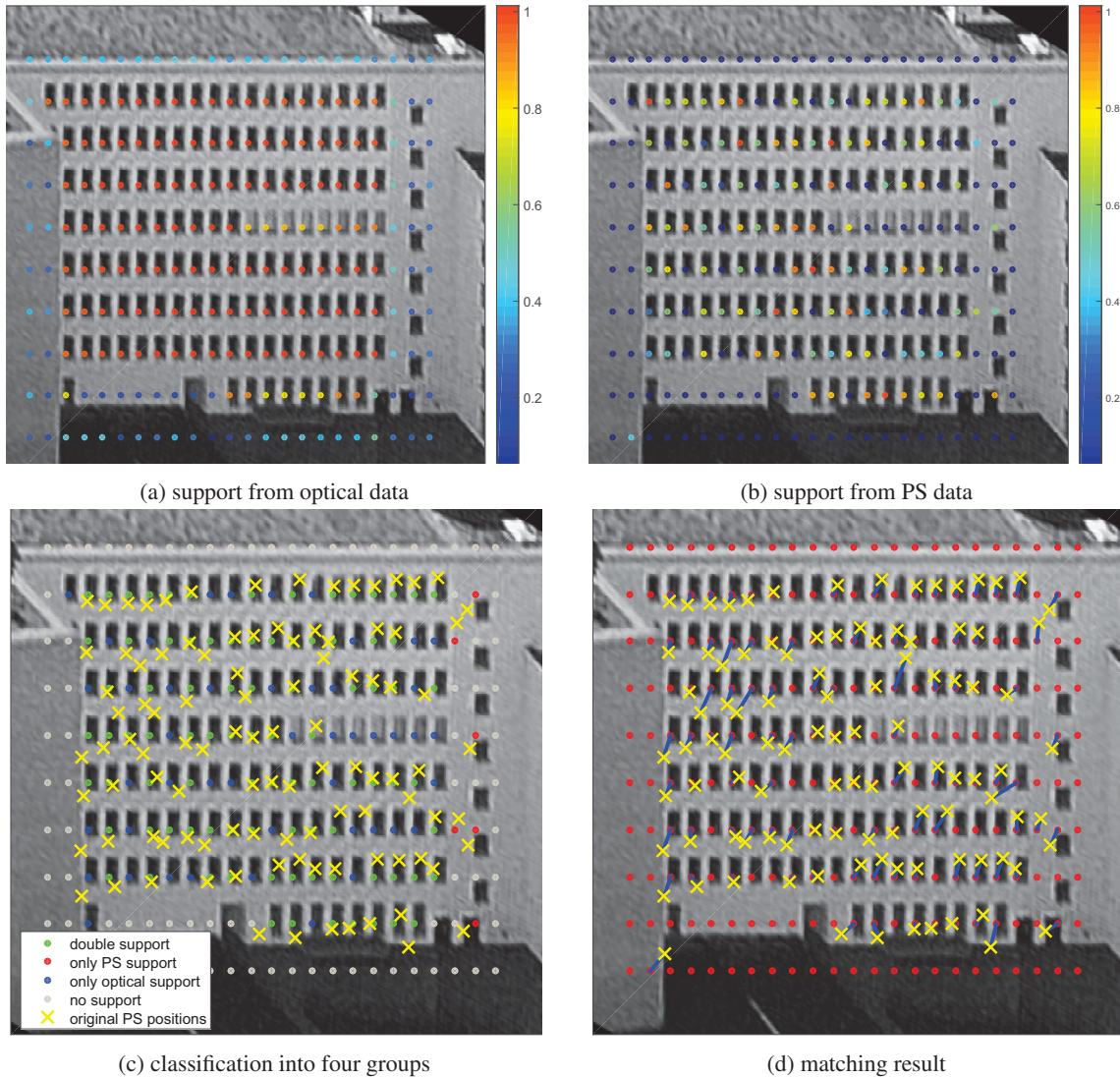
(a) support from optical data

(b) support from PS data

- ● double support
- ● only PS support
- ● only optical support
- ● no support
- ✕ original PS positions

(c) classification into four groups

(d) matching result

Figure 6: Result for case study 'Lindenstrasse 69'. (a) - (d) similar to Fig. 5.

5.2. Lindenstrasse 69

The building Lindenstrasse 69 is an office building with 8 floors. The facade is characterized by regularly aligned windows which are displaced inside the building face. Figure 6 shows results analog to the case study 'Axel-Springer building'. An interesting detail can be seen on the right hand side in the middle section of the facade. A horizontal group of six PS are missing resulting in a low support score from the PS data (compare Figure 6c and 6b). Figure 6a shows that this area also exhibits a low optical support. This suggests the assumption that the facade structure in this area is different compared to the surrounding leading to an unlike appearance in the optical image as well a different reflection mechanism resulting in the absence of PS.

6. Conclusion

We presented a first comprehensive process of accurately projecting Persistent Scatterer into oblique optical images and assigning them to a regular lattice. The presented approach uses a model which describes PS at a facade as regularly spaced points in a plane. Establishing the connection between grouped PS and optical imagery forms a tool for investigating the reflection mechanisms. The lattice information, for example, can be used in the PS processing as additional information to support their detection. The used model restricts the approach to a very limited subset of existing facades. The assignment of PS to optical lattices can only be performed if both data exhibit an regularly spaced lattice distribution. Further work will comprise the extension of the presented approach towards a more general facade model, like for instance, grammar-based methods.

References

[1] S. Auer. *3D Synthetic Aperture Radar Simulation for Interpreting Complex Urban Reflection Scenarios*. PhD thesis, Technische Universität München, Faculty of Civil, Geo and Environmental Engineering, 2011. 1

[2] R. Bamler and M. Eineder. Accuracy of Differential Shift Estimation by Correlation and Split-Bandwidth Interferometry for Wideband and Delta-k SAR Systems. *IEEE Geoscience and Remote Sensing Letters*, 2(2):151–155, Apr. 2005. 1

[3] R. Bamler, M. Eineder, N. Adam, X. X. Zhu, and S. Gernhardt. Interferometric Potential of High Resolution Spaceborne SAR. *PFG Photogrammetrie - Fernerkundung - Geoinformation*, 2009(5):407–419, Nov. 2009. 1, 3

[4] K. Chureesampant and J. Susaki. Land cover classification using multi-temporal SAR data and optical data fusion with adaptive training sample selection. In *2012 IEEE International Geoscience and Remote Sensing Symposium*, pages 6177–6180. Ieee, July 2012. 2

[5] M. Crosetto, O. Monserrat, and G. Herrera. Urban applications of persistent scatterer interferometry. In U. Soergel, editor, *Radar Remote Sensing of Urban Areas*, volume 15 of *Remote Sensing and Digital Image Processing*, pages 233–248. Springer Netherlands, 2010. 2

[6] A. Ferretti, C. Prati, and F. Rocca. Permanent Scatterers in SAR interferometry. *IEEE Transactions on Geoscience and Remote Sensing*, 39(1):8–20, 2001. 1

[7] M. a. Fischler and R. C. Bolles. Random sample consensus: a paradigm for model fitting with applications to image analysis and automated cartography. *Communications of the ACM*, 24(6):381–395, 1981. 4

[8] S. Gernhardt, S. Auer, and K. Eder. Persistent scatterers at building facades Evaluation of appearance and localization accuracy. *ISPRS Journal of Photogrammetry and Remote Sensing*, 100:92–105, June 2014. 2

[9] J. C. Lagarias, J. Reeds, M. H. Wright, and P. E. Wright. Convergence Properties of the Nelder–Mead Simplex Method in Low Dimensions. *SIAM Journal on Optimization*, 9(1):112–147, 1998. 6

[10] P. C. Mahalanobis. On the generalised distance in statistics. *Proceedings of the National Institute of Sciences of India*, 2:49–55, 1936. 5

[11] E. M. Mikhail and F. E. Ackermann. *Observations and Least Squares*. The University of Michigan, University Press of America, illustrated edition, Nov. 1982. 3

[12] J. Munkres. Algorithms for the assignment and transportation problems. *Journal of the Society for Industrial and Applied Mathematics*, 5(1):32–38, 1957. 2

[13] N. Otsu. A threshold selection method from gray-level histograms. *IEEE Transactions on Systems, Man and Cybernetics*, 9(1):62–66, 1979. 6

[14] L. Schack and U. Soergel. Exploiting Regular Patterns to Group Persistent Scatterers in Urban Areas. *IEEE Journal of Selected Topics in Applied Earth Observations and Remote Sensing*, 7(10):4177–4183, 2014. 3

[15] A. Schunert and U. Soergel. Grouping of Persistent Scatterers in high-resolution SAR data of urban scenes. *ISPRS Journal of Photogrammetry and Remote Sensing*, 73:80–88, Sept. 2012. 2, 4

[16] J. Wegner, J. Inglada, and C. Tison. Automatic Fusion of SAR and Optical Imagery based on Line Features. In *European Conference on Synthetic Aperture Radar*, pages 171–174, 2008. 2

[17] M. Xu, Z. Xia, F. Zhang, K. Li, and C. Xie. Multi-Temporal Polarimetric SAR and Optical Data Fusion for Land Cover Mapping in Southwest China. In *International Conference on Multimedia Technology (ICMT) 2010*, pages 1–4, 2010. 2